Polymers **2011**, *3*, 1565-1574; doi:10.3390/polym3031565

OPEN ACCESS

polymers

ISSN 2073-4360

www.mdpi.com/journal/polymers

Article

Loading of Two Related Metal-Organic Frameworks (MOFs), $[Cu_2(bdc)_2(dabco)]$ and $[Cu_2(ndc)_2(dabco)]$, with Ferrocene

Romain Heck [1], Osama Shekhah [1], Olexandra Zybaylo [1], Peter G. Weidler [1], Frank Friedrich [1], Robert Maul [2,3], Wolfgang Wenzel [4] and Christof Wöll [1,*]

[1] Institut für Funktionelle Grenzflächen, Karlsruher Institut für Technologie, Hermann-von-Helmholtz-Platz 1, B 330, D-76344 Eggenstein-Leopoldshafen, Germany; E-Mails: Romain. Heck@kit.edu (R.H.); osama.shekhah@kit.edu (O.S.); olexandra.zybaylo@kit.edu (O.Z.); peter.weidler@kit.edu (P.G.W.); frank.friedrich@kit.edu (F.F.)

[2] Steinbuch Center for Computing, Karlsruher Institut für Technologie (KIT), Karlsruhe 76021, Germany; E-Mail: robert.maul@kit.edu (R.M.)

[3] DFG Center for Functional Nanostructures, Karlsruher Institut für Technologie (KIT), Karlsruhe 76021, Germany

[4] Institut für Nanotechnology (INT), Karlsruher Institut für Technologie (KIT), Karlsruhe 76021, Germany; E-Mail: wolfgang.wenzel@kit.edu (W.W.)

* Author to whom correspondence should be addressed; E-Mail: Christof.Woell@kit.edu; Tel.: +49-724-782-3934; Fax: +49-724-782-3478.

Received: 9 July 2011; in revised form: 30 August 2011 / Accepted: 20 September 2011 / Published: 21 September 2011

Abstract: We have studied the loading of two related, similar porous metal-organic frameworks (MOFs) $[Cu_2(bdc)_2(dabco)]$ (**1**), and $[Cu_2(ndc)_2(dabco)]$ (**2**) with ferrocene by exposing bulk powder samples to the corresponding vapor. On the basis of powder X-ray diffraction data and molecular dynamics (MD) calculations we propose that each pore can store one ferrocene molecule. Despite the rather pronounced similarity of the two MOFs a quite different behavior is observed, for **1** loading with ferrocene leads to an anisotropic 1% contraction, whereas for **2** no deformation is observed. Mössbauer spectroscopy studies reveal that the Fe oxidation level remains unchanged during the process. Time dependent studies reveal that the diffusion constant governing the loading from the gas-phase for **1** is approximately three times larger than the value for **2**.

Keywords: ferrocene; loading; MOFs

1. Introduction

Metal-organic frameworks (MOFs) are 3D porous coordination polymers self-assembled from metal ions salts and organic linkers. Their porosity, and in particular the possibility to functionalize the organic linkers before or after the assembly of the framework, generate a large number of potential applications such as gas storage and separation, sensors, catalysis and drug delivery [1]. So far, loading studies of MOFs have largely focused on small molecules like H_2, CO, CO_2, *etc.* [2]; for larger molecules like benzene or pyridine [3] the number of available studies is limited. For even larger molecules like ferrocene, which become comparable in size to the pores within MOFs, only a relatively small number of works have been reported. Nevertheless, in particular for the redox-active ferrocene there are a number of interesting applications, as demonstrated by a recent study from Fischer and co-workers, who have studied the redox properties of a ferrocene derivative embedded inside the pores of a MOF [4-6]. They have demonstrated that after loading of a particular MOF (MIL-53) the systems exhibits catalytic properties with regard to the selective oxidation of benzene to phenol in the presence of aqueous hydrogen peroxide. This result reveals that the redox properties of ferrocene embedded inside MOFs are very interesting from a chemical point of view and also carries a substantial potential with regard to the synthesis of sensors or electrode materials. Following this line of thought, we have carried out a systematic investigation of the loading of ferrocene into two homostructural MOFs: $[Cu_2(bdc)_2(dabco)]$ (**1**), (bdc: benzene dicarboxylate dabco, 1,4-diazabicyclo-[2.2.2]octane) and $[Cu_2(ndc)_2(dabco)]$ (**2**), (ndc: 1,4-naphthalene-dicarboxylate) [7], using X-ray diffraction and Mössbauer spectroscopy.

2. Results and Discussion

*2.1. Loading of Ferrocene in $[Cu_2(bdc)_2(dabco)]$ (**1**) and $[Cu_2(ndc)_2(dabco)]$ (**2**)*

The successful loading of ferrocene inside both frameworks was evident immediately, after exposure to ferrocene vapor, the light blue powder turned a dull green in the case of **1**, and the light green powder turned a dull darker green in the case of **2**. The embedding of ferrocene was confirmed by elemental analysis and EDX (Table 1). Whereas for **1** the analytical results are consistent with roughly 1 ferrocene per pore, for **2** the amount of ferrocene is only about 50% of that seen for **1**, revealing that the total amount of included ferrocene is substantially smaller.

Table 1. Evaluation of the ferrocene content inside $[Cu_2(bdc)_2(dabco)]$ (**1**) and $[Cu_2(ndc)_2(dabco)]$ (**2**).

1	-	**# ferrocene/unit cell**
EDX (Fe wt%)	7.00	1.38
Microanalysis (%)	1.23	1.28
2	-	
EDX (Fe wt%)	2.54	0.51
Microanalysis (%)	0.57	0.64

Figure 1. Monitoring with PXRD of the loading of ferrocene inside Cu(bdc)(dabco)$_{1/2}$ (**1**) and Cu(ndc)(dabco)$_{1/2}$ (**top**) (**2**) and compared to the theoretical calculations for both types of MOFs after loading with ferrocene (**bottom**).

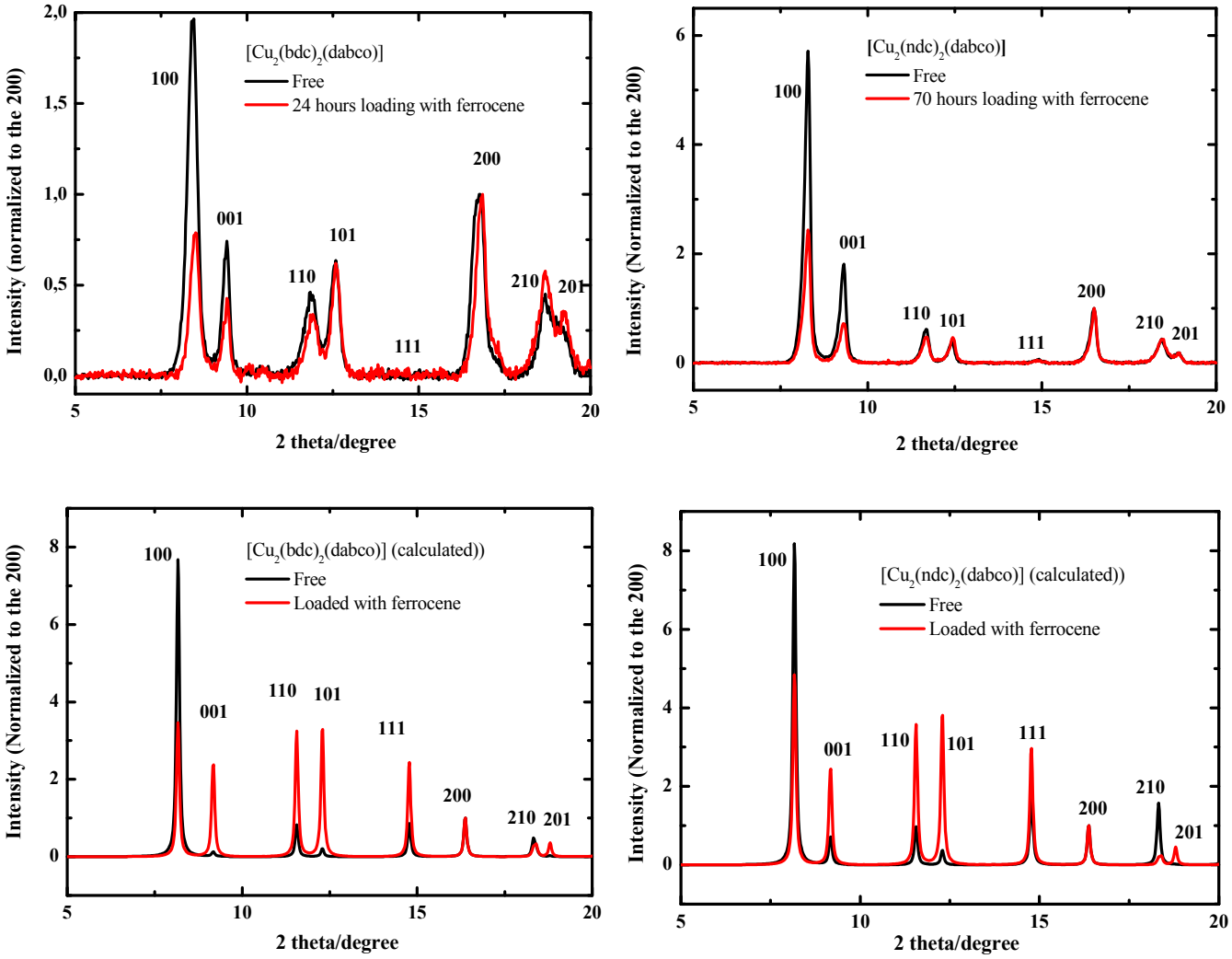

In order to demonstrate that the ferrocene molecules are loaded inside the MOF pores and to rule out that the signal detected in the elemental analysis results from small ferrocene particles nucleated at the outer surface of the MOF powder particles we have carried out PXRD-studies. The loading of ferrocene into **1** and **2** dried bulk powders was done inside a closed dome, under an overall pressure of 1 atmosphere (the partial vapor pressure of ferrocene at 293 K amounts to 1 Pa. [9]) and was monitored by PXRD as shown in Figure 1. After exposing to ferrocene vapor, we observe an overall reduction in the relative intensities of the diffraction peaks. In order to make this important effect more visible we have normalized all X-ray diffraction data to the (200) peak. According to the calculated XRD patterns the intensity of this peak is not affected by loading the MOF lattice with one ferrocene molecule per pore (see Figure 1, bottom). A rationalization of these strong intensity changes for the (100)-peak, but not for the (200) peak, is provided below. The strong change in the relative intensity of the (200) and (100) peak clearly reveals that ferrocene is loaded inside the pores of the two different MOFs. In the case of **1**, a small shift of the peak positions ((100), (110),..) towards higher diffraction angles is seen, whereas for **2** no significant change of the peak position was observable. The loss of peak intensities after 24 h of loading is most pronounced for the (100) and (001) reflections. A detailed

analysis of the peak positions reveals an anisotropic contraction of the framework in the case of **1**, the a and b axis are reduced from 1.0597 ± 0.0004 nm to 1.0510 ± 0.0008 nm while the c axis undergoes a small increase from 0.9491 ± 0.0008 nm to 0.9482 ± 0.0010 nm. The symmetry of the framework however remains unchanged at the applied tetragonal space group P4. The overall effect of ferrocene loading results in a volume decrease of the pores from 1.065 nm^3 to 1.047 nm^3. The somewhat unexpected contraction of **1** can be rationalized by considering that this MOF structure is not as rigid as in the case of **2**. Apparently this flexibility allows for a small contraction for the maximization of π-p interaction between the η^5-C_5H_5 moieties of the ferrocene and the aromatic cores of the linkers of the **1**. PXRD data recorded after unloading the MOF-lattice were very similar to the original data recorded for the empty material, demonstrating that the contraction of the lattice upon loading with ferrocene is reversible.

A quite similar behavior is seen in the case of **2**. Although in this case we observe an overall reduction of all diffraction peaks, again normalization to the (200) peak reveal a substantial change in the relative intensities of the form factors. As in the case of [1] this change in the form factor clearly reveals that ferrocene is loaded inside the MOF pores. Inspection of the PXRD-data (Figure 1) reveals that all peaks are at the same position of the pristine powder, which indicates that no contraction or change in the symmetry of the crystals happens due to the rigidity of **2** [11].

In order to elucidate the position and the orientation of the ferrocene molecules hosted within the pores of the MOF on the atomic level we have employed molecular dynamics simulations (MD) using the Amber10 molecular modeling package using the GAFF force field [12]. The MD simulations were carried out for a temperature of 300 K Simulation time was 2.0 ns, and the increment amounted to 0.5 fs. As a starting point for the calculations we used a $[Cu_2(bdc)_2(dabco)]$ framework with the known bulk structure parameters. After adding the ferrocene inside the centre of a pore the geometry of the system was optimized with respect to the total energy. During the simulations also the dynamics of the added molecule interacting with the backbone of the framework was monitored. During the molecular dynamics simulation the unit cell corners of the MOF lattice were kept fixed at their equilibrium positions. In Figure 2 we display a snapshot of the conformation of ferrocene inside the pore. As a result of the competing effects of non-covalent interactions between ferrocene and the benzene ring-units of the MOF structure and steric repulsion we observe a weak binding of the ferrocene molecule to the backbone of the framework. The interaction energy between ferrocene and a benzene ring-unit of the MOF was found to amount to −12.16 kcal/mol, a value which is in line with that expected for π-π-stacking effects occurring between the neutral benzene ring of the framework and the partially charge cyclopentadienyl rings of ferrocene.

The overall integrity of the frameworks after loading has been checked microscopically by SEM. The images show that the crystallites of [(η5-C5H5)2Fe] 0.08@ [Cu2(bdc)2(dabco)] (**3**) and [(η5-C5H5)2Fe] 0.04@ [Cu2(ndc)2(dabco)] (**4**) are still intact after 92 hours of loading (Figure 3). Moreover the reversibility of the loading of ferrocene has been checked by putting a sample of **1** under high-vacuum for 4 h and measuring its PXRD pattern afterwards. The structure of the material is essentially unchanged even though it underwent some small deterioration, with a higher general background. However all the diffraction peaks went back to their original position showing that the framework re-expands upon ferrocene evaporation. The broadening of the individual XRD-peaks and the

increase in background must be due to the strain generated on the framework by the cycles of loading and de-loading of ferrocene inside of it generating some defects within the crystallites.

Figure 2. Geometry of $[Cu_2(bdc)_2(dabco)]$ (**1**) after the embedding of one molecule of ferrocene per unit cell, as obtained from MD-simulations. The grey surface indicates the free space in the unit cell of the empty MOF before the loading process. White: hydrogen, teal: carbon, red: oxygen, purple: nitrogen, teal: copper, green: Ferrocene.

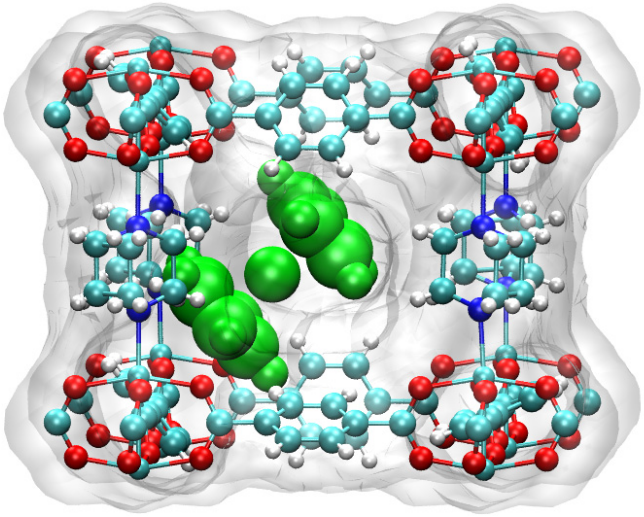

Figure 3. SEM pictures of $[(\eta^5\text{-}C_5H_5)_2Fe]$ 0.08@ $[Cu_2(bdc)_2(dabco)]$ (**3**) (**left**) $[(\eta^5\text{-}C_5H_5)_2Fe]$ 0.04@ $[Cu_2(ndc)_2(dabco)]$ (**4**) (**right**).

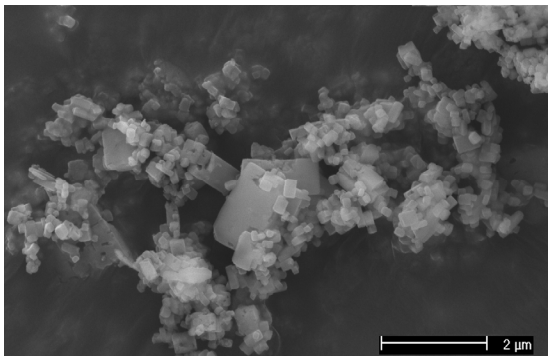

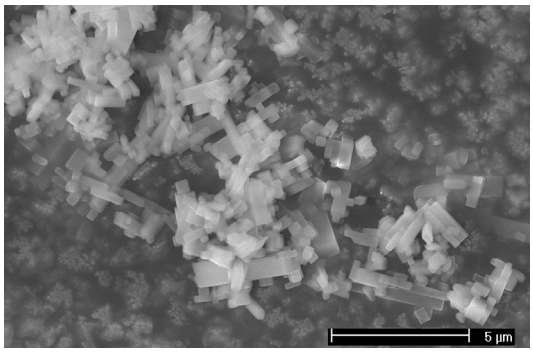

The fact that after loading with ferrocene the simulated XRD patterns show strong changes for the (100) and (001) (h + k + l = odd) peaks, whereas the (002) and (101) peaks reveal small changes in intensity only can be rationalized by considering a hypothetical structure where the Cu dimers at the corners of the Cu-bdc-dabco unit cells are replaced by a single Cu atom. Neglecting the other atoms in the MOF-lattice (which have a much smaller scattering cross sections for x-rays that the metal atoms) then yields a tetragonal, primitive P4 structure. If, in such a structure, a Cu atom is placed at center of the P4 unit cell, we obtain a centered I4 lattice. The extinction rules for such a body centered lattice require the reflections with an odd sum of h + k + l to disappear. Although the atomic scattering amplitude of Fe is approximately 1/3 larger than that of Cu this consideration nicely explains why the intensites of the (100) and (001) peaks show a strong decrease upon loading the MOF with ferrocene, whereas the peaks with h + k + l equal an even number show no, or only a very slight, intensity changes. The same considerations apply for Fc loaded into the Cu(ndc)dabco lattice.

2.2. Mössbauer Study

In the case of iron a convenient way to check the oxidation state of the corresponding binds is to apply Mössbauer spectroscopy. It is one of the most sensitive techniques in terms of energy resolution and capability of detecting changes in the energy levels of an atomic nucleus in response to its environment. It is based on the recoil-free, resonant absorption and emission of gamma rays in solids [13], After loading the two types of MOFs. studied here with ferrocene in both cases a doublet was obtained (Figure 4) with δ and ΔE_q values of 0.535 mm/s and 2.423 mm/s, respectively, in the case of **3** and with the δ and ΔE_Q values of 0.554 mm/s and 2.447 mm/s, respectively, in the case of **4**. All peak positions are characteristic for Fe^{II} low-spin of the ferrocene unit. And these data demonstrate that the level of oxidation of the iron in the ferrocene remains unchanged after its diffusion inside both frameworks and that no redox reaction takes place between the frameworks (either with the aromatic linkers or with the metal clusters) and the embedded ferrocene. We can thus safely conclude that all the changes observed in both materials were only due to the steric interactions and strain generated by the ferrocene molecules diffusing through their pores. These results also imply that the ferrocene embedded in the MOF pores is available to undergo redox reactions. This option will be explored in future work.

Figure 4. Mössbauer Spectra of ferrocene embedded in $[Cu_2(ndc)_2(dabco)]$.

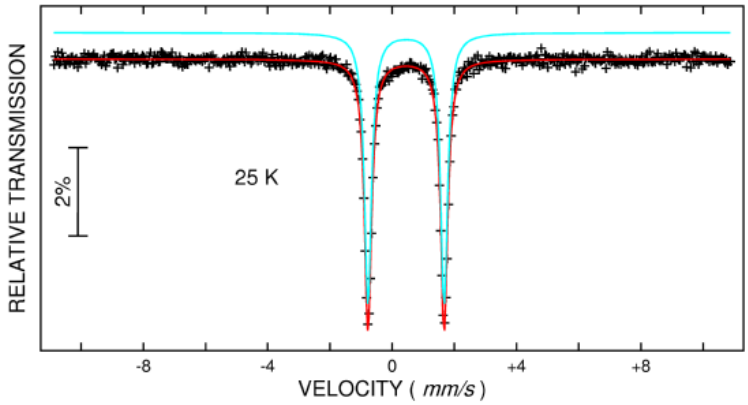

2.3. Kinetic Studies

Both frameworks were used as-made for the kinetic studies without being evacuated or having undergone any pre-treatment. To this and the kinetics of diffusion of ferrocene inside [**1**] and [**2**] were monitored over time with PXRD. The decreasing intensity of the (100) Bragg-peak was used as a probe in both cases. The natural logarithm of the resulting peak intensities were plotted against time of exposure (Figure 5). Both incorporations showed similar kinetics but the diffusion constants obtained from the plot of ln(intensity) against time D was 0.062 ± 0.001 for **1** and 0.022 ± 0.001 **2**. Both linear regressions exhibited high correlation coefficients R^2 of 0.995 and 0.999 respectively.

The speed of diffusion is favored by the openness of the pores, the interactions of the η^5-C_5H_5 moieties with the aromatic cores of the bdc forming the skeleton of the framework and the fact that ferrocene is small enough to be freely flowing through the channels (ferrocene: 2.79 Å × 2.67 Å, pore window: 7.13 Å × 5.63 Å).

Figure 5. Kinetics of the loading of ferrocene inside Cu(bdc)(dabco)$_{1/2}$ (**1**) (□) and Cu(ndc)(dabco)$_{1/2}$ (**2**) (○). The data are plotted as the natural log of intensity against time to obtain diffusion constants.

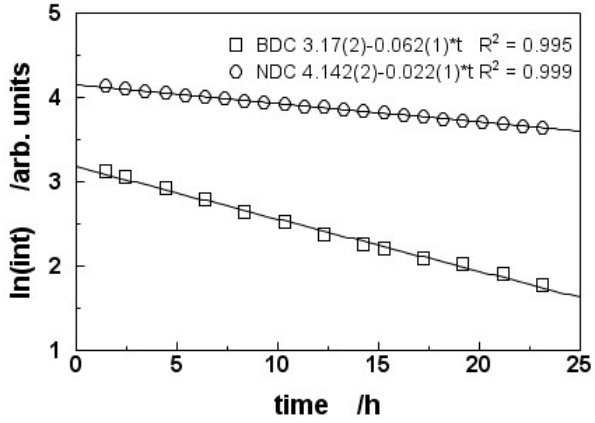

In the case of **2** the kinetics is for almost a factor of 3 slower. This rather slow diffusion of ferrocene in **2** is consistent with the fact that due to the bulkiness of the ndc ligand the channels within **2** are substantially smaller than in **1**. This can explain the difference in kinetics of diffusion between **1** and **2**, ndc linkers having to rotate and to slightly move away from each other, thus forcing a phase transition within the framework and allowing for a smooth diffusion of ferrocene throughout it. This process becomes more and more difficult as more and more ferrocene is embedded in the framework and needs a longer time for completion.

3. Experimental Section

3.1. Synthesis

All solvents, organic linkers and metal salts were purchased from Aldrich and were used as received. The [Cu_2(bdc)$_2$(dabco)] and [Cu_2(bdc)$_2$(dabco)] materials were synthesized according to the scheme described in the literature [8], the samples were purified by repeated washing with DMF and ethanol and finally dried in air. The characterization was done by PXRD, elemental analysis and Mössbauer spectroscopy.

[Cu_2(bdc)$_2$(dabco)] (**1**)

A mixture of Cu(CH_3CO_2)$_2$,H_2O (0.670 g, 3.36 mmol), H_2bdc (0.506 g, 3.37 mmol) and dabco (0.187 g, 1.67 mmol) was suspended in DMF (40 mL) and heated in a sealed glass vessel at 120 °C for 2 days. The light blue crystalline precipitate formed was collected, washed with DMF and dried at 100 °C for 48 hours. Elemental analysis calculated for [Cu($C_8H_4O_4$)($C_6H_{12}N_2$)$_{0.5}$] • 0.4 (DMF) • 1.7 (H_2O): C 42.64, H 4.75, N 5.71; found: C 42.70, H 4.86, 5.75.

[Cu_2(ndc)$_2$(dabco)] (2)

A mixture of $Cu(CH_3COO)_2,H_2O$ (0.670 g, 3.36 mmol), H_2ndc (0.728 g, 3.37 mmol) and dabco (0.187 g, 1.67 mmol) was suspended in DMF (40 mL), sonicated for 30 min and heated in a sealed glass vessel at 120 °C for 2 days. The light green crystalline precipitate formed was collected, washed with DMF and ethanol and dried dried at 100 °C for 48 hours. Elemental analysis calculated for $[Cu(C_{10}H_6O_4)(C_6H_{12}N_2)_{0.5}]$ • 0.6 (EtOH) • 1.6 (H_2O): C 49.85, H 4.85, N 3.59; found: C 49.8, H 4.86, N 3.64.

[(η^5-C_5H_5)$_2$Fe] 0.08@ [Cu_2(bdc)$_2$(dabco)] (3)

100 mg of dried **1** was placed on a watch glass in a sealed glass vial containing 1g of ferrocene and left standing at room temperature for 3 days. The light blue crystalline turned dull green. Elemental analysis calculated for $[(\eta^5\text{-}C_5H_5)_2Fe]_{0.08}@[Cu(C_8H_4O_4)(C_6H_{12}N_2)_{0.5}]$ • 0.4 (DMF) • 1.8 (H_2O): C 43.3, H 4.81, N 5.44; found: C 43, H 4.4, N 5.76.

[(η^5-C_5H_5)$_2$Fe] 0.04@ [Cu_2(ndc)$_2$(dabco)] (4)

100 mg of dried **2** was placed on a watch glass in a sealed glass vial containing 1g of ferrocene and left standing at room temperature for 3 days. The light green crystalline turned dull green. Elemental analysis calculated for $[(\eta^5\text{-}C_5H_5)_2Fe]$ 0.04@$[Cu(C_{10}H_6O_4)(C_6H_{12}N_2)_{0.5}]$ • 0.3 (EtOH) • 1.7 (H_2O): C 49.8, H 4.59, N 3.63; found: C 49.6, H 4.54, N 3.84.

3.2. Analytical Methods, PXRD, SEM, Elemental Analysis, Mössbauer Spectroscopy

The following routine methods were employed: Powder X-Ray Diffraction (PXRD) of the samples was recorded with a D8-Advance diffractometer by (Bruker AXS) with Cu Kα-radiation (l = 1.5418 Å) in Bragg-Brentano θ–2θ geometry and with a LynxEye© 1-dim compound silicon strip detector. Scan range was from 5–45°2θ, 89 seconds counting time per 0.024°2θ step. The (111) Bragg peak of the gold substrate was used as internal standard for sample height corrections. C, H, N analyses were carried out using a LECO Mirco TrueSpec CHNS instrument. Iron analysis was done by dissolving the material with acid and pressure in a Microwave and analyzing the solution with an ICP-OES from Varian Inc. Corporation. The Mössbauer spectra were acquired using a conventional spectrometer in the constant-acceleration mode equipped with a ^{57}Co source (3.7 GBq) in rhodium matrix. Isomer shifts are given relative to α-Fe at room temperature. The sample was inserted inside an Oxford Instruments Mössbauer-Spectromag 4000 Cryostat. The sample temperature can be varied between 3.0 and 300 K. Mössbauer spectra were evaluated by using the NORMOS package program.

3.3. Kinetic Studies

Both materials **1** and **2** were dried and loaded on the PXRD stage under a close dome in the presence of ferrocene powder. The vapor pressure of ferrocene at 293 K amounts to 1 Pa [9]. The loading of ferrocene inside the frameworks was followed over 24 h by PXRD. The kinetic data was extracted from the natural logarithm of the intensity of the (100) Bragg peak after background

subtraction and plotting against time of exposure of the material to ferrocene vapours. The data was then fitted by a linear regression and the diffusion constant D was obtained from the slope obtained by the fit [10].

4. Conclusions

We have successfully demonstrated that ferrocene can be embedded into two types of related MOFs, $[Cu_2(bdc)_2(dabco)]$ (**1**) and $[Cu_2(ndc)_2(dabco)]$ (**2**) by simple exposure to ferrocene vapor. Moreover, we have seen that the bulkiness of the ndc ligand leads to a much slower diffusion of ferrocene inside the framework. The loading is accompanied by a small, anisotropic contraction in case of **1**, whereas no deformation is observed in the case of **2**. Finally, we were able to demonstrate that ferrocene did not undergo any redox chemistry upon inclusion thus making it available as a redox active site, e.g., for potential selective catalytic transformations.

Acknowledgments

Funding from the German DFG through SPP 1362 is gratefully acknowledged. We thank V.V. Mereacre from the (Institut für Anorganische Chemie-KIT) for recording the Mössbauer spectra.

References

1. Kuppler, R.J.; Timmons, D.J.; Fang, Q.R.; Li, J.R.; Makal, T.A.; Young, M.D.; Yuan, D.Q.; Zhao, D.; Zhuang, W.J.; Zhou, H.C. Potential applications of metal-organic frameworks. *Coord. Chem. Rev.* **2009**, *253*, 3042-3066.
2. Bordiga, S.; Regli, L.; Bonino, F.; Groppo, E.; Lamberti, C.; Xiao, B.; Wheatley, P.S.; Morris, R.E.; Zecchina, A. Adsorption properties of HKUST-1 toward hydrogen and other small molecules monitored by IR. *Phys. Chem. Chem. Phys.* **2007**, *9*, 2676-2685.
3. Zybaylo, O.; Shekhah, O.; Wang, H.; Tafipolsky, M.; Schmid, R.; Johannsmann, D.; Wöll, C. A novel method to measure diffusion coefficients in porous metal-organic frameworks. *Phys. Chem. Chem. Phys.* **2010**, *12*, 8092-8097.
4. Meilikhov, M.; Yusenko, K.; Fischer, R.A. Incorporation of metallocenes into the channel structured Metal-Organic Frameworks MIL-53(Al) and MIL-47(V). *Dalton Trans.* **2010**, *39*, 10990-10999.
5. Meilikhov, M.; Yusenko, K.; Fischer, R.A. Turning MIL-53(Al) redox-active by functionalization of the bridging OH-group with 1, 1'-ferrocenediyl-dimethylsilane. *J. Am. Chem. Soc.* **2009**, *131*, 9644-9645.
6. Meilikhov, M.; Yusenko, K.; Torrisi, A.; Jee, B.; Mellot-Draznieks, C.; Poppl, A.; Fischer, R.A. Reduction of a metal organic framework by an organometallic complex: Magnetic properties and structure of the inclusion compound [(eta(5)-C_5H_5)(2)Co](0.5)@MIL-47(V). *Angew. Chem. Int. Ed.* **2010**, *49*, 6212-6215.
7. Kitagawa, S.; Kitaura, R.; Noro, S. Functional porous coordination polymers. *Angew. Chem. Int. Ed.* **2004**, *43*, 2334-2375.

8. Dybtsev, D.N.; Chun, H.; Kim, K. Rigid and flexible: A highly porous metal-organic framework with unusual guest-dependent dynamic behavior. *Angew. Chem. Int. Ed.* **2004**, *43*, 5033-5036.
9. Monte, M.J.S.; Santos, L.; Fulem, M.; Fonseca, J.M.S.; Sousa, C.A.D. New static apparatus and vapor pressure of reference materials: Naphthalene, benzoic acid, benzophenone, and ferrocene. *J. Chem. Eng. Data* **2006**, *51*, 757-766.
10. Jost, W.; Hauffe, K. *Diffusion, Methoden Der Messung und Auswertung*; Steinkopff Verlag: Darmstadt, Geramny, 1972; p. 327.
11. Furukawa, S.; Hirai, K.; Nakagawa, K.; Takashima, Y.; Matsuda, R.; Tsuruoka, T.; Kondo, M.; Haruki, R.; Tanaka, D.; Sakamoto, H.; *et al.* Heterogeneously hybridized porous coordination polymer crystals: Fabrication of heterometallic core-shell single crystals with an in-plane rotational epitaxial relationship. *Angew. Chem. Int. Ed.* **2009**, *48*, 1766-1770.
12. Case, D.A.; Cheatham, T.E.; Darden, T.; Gohlke, H.; Luo, R.; Merz, K.M.; Onufriev, A.; Simmerling, C.; Wang, B.; Woods, R.J. The Amber biomolecular simulation programs. *J. Comput. Chem.* **2005**, *26*, 1668-1688.
13. Clark, S.J.; Donaldson, J.D.; Thomas, M.J.K. Moessbauer Spectroscopy. In *Spectroscopic Properties of Inorganic and Organometallic Compounds*; Davidson, G., Ebsworth, E.A.V., Eds.; Specialist Periodical Reports; Royal Society of Chemistry: Cambridge, UK, 1989; Volume 22, pp. 363-461.